Trans. Phenom. Nano Micro Scales, 4(2): 1-8, Winter - Spring 2016
DOI: 10.7508/tpnms.2016.02.001

ORIGINAL RESEARCH PAPER

Thermo-mechanical properties of polymer nanocomposites reinforced with randomly distributed silica nanoparticles- Micromechanical analysis

R. Ansari [1]***, M.K. Hassanzadeh Aghdam*** [1,*]

[1]*Department of Mechanical Engineering, University of Guilan, P.O. Box 3756, Rasht, I. R.Iran*

Received 22 May 2015; revised 15 December 2015; accepted 20 December 2015; available online 28 June 2016

ABSTRACT: A three-dimensional micromechanics-based analytical model is developed to study thermo-mechanical properties of polymer composites reinforced with randomly distributed silica nanoparticles. Two important factors in nanocomposites modeling using micromechanical models are nanoparticle arrangement in matrix and interphase effects. In order to study these cases, representative volume element (RVE) of nanocomposites is extended to $c\times r\times h$ nano-cells in three dimensions and consists of three phases including nanoparticles, polymer matrix and interphase between the nanoparticles and matrix. Nanoparticles are surrounded by the interphase in all composites. Effects of volume fraction, aspect ratio and size of nanoparticle on the effective thermo-mechanical response of the nanocomposite are studied. Also, the effects of polymer matrix properties and interphase including its elastic modulus and thickness are theoretically investigated in detail. It is revealed that when nanoparticles are randomly distributed in the matrix and interphase effects are considered, the results of present micromechanical model are in very good agreement with experimental data.

KEYWORDS: *Interphase; Micromechanics; Nanocomposite; Random distribution; Thermo-mechanical properties*

INTRODUCTION

Nanocomposites are a new class of composite materials in which the reinforcing phase sizes are in the order of nanometer [1-2]. Adding nanofillers to polymers can result in significant improvement to mechanical, thermal and electrical properties at relatively small volume or weight fractions of nanofiller [3-7]. For these reasons, they are commonly used in aerospace industry, automobile manufacturing and medical devices [8]. Moreover, for accurate application and a reliable and optimal design, knowing structure-property relationships for nanocomposites modeling is very important. It is well-known that two factors play significant role in nanocomposite materials modeling, interphase effects and nanofillers distribution [9-13]. The interphase region is a unique characteristic of nanocomposites as compared to usual composites with micro constituents. This is an area of matrix material inclosing the nanofiller that has distinct properties from those of the bulk matrix. Also, the number density of nanofiller in a polymer matrix is greater than that of microscale filler in a polymer matrix which makes filler spacing and its arrangement critical factors in composite design. Furthermore, in practice, the state of distribution of nanofillers in the matrix is random, but in some of micromechanical modeling it is assumed to be repeating [14-15]. There are many methods such as finite elements (FE) and analytical micromechanics models in order to predict the overall behavior of usual composites with micro-scale reinforcement [16-22].

Some of these analytical micromechanics and finite elements models were recently utilized to predict the overall stiffness of nanocomposites [14-15, 23-27]. Also, in order to investigate nanocomposite systems, computational modeling techniques based on molecular dynamics approaches were used [28-30]. Although, there are some studies on stiffness of nanocomposites using both finite elements and analytical micromechanics models, the general modeling of thermo-mechanical properties of the nanocomposites with considering effects of arrangement of nanofiller, nanofiller geometry and interphase using a micromechanics-based analytical model has not been studied in the published literature.

In this work, the modified version of Simplified unit cell (SUC) micromechanical model [16, 31] is applied to obtain thermo-elastic properties of nanocomposites. The most important advantages of this new model are its accuracy, simplicity, and efficiency. Using the micromechanical model, the effects of random nanofiller arrangement, nanofiller geometry and interphase on the thermo-mechanical properties of nanocomposites are studied. The geometry of the RVE of SUC model is extended to $c\times r\times h$ nano-cells in three dimensions in order to cover a more realistic geometry of the nanocomposites and also to supply more accurate approximation of the thermo-elastic properties of the nanocomposites.

The nanoparticle, interphase and matrix materials are supposed to be homogeneous and isotropic too. Furthermore, a perfectly bonded interface is assumed between the nanoparticle, interphase and matrix. Presented

*Corresponding Author Email: *mk.hassanzadeh@gmail.com*
Tel.: +981426584365; Note. This manuscript was submitted on May 22, 2015; approved on December 15, 2015; published online June 28, 2016.

Nomenclature

		S	Elastic compliance matrice
L_C	lengths of the RVE in the x direction (nm)	A	Coefficients matrice
L_r	lengths of the RVE in the y direction(nm)	F	External load vector (nN)
L_h	lengths of the RVE in the z direction (nm)		**Greek Symbols**
a_i	length of each cell in the x direction (nm)	σ_x	Local stress in the x direction (nN/nm^2)
b_j	length of each cell in the y direction (nm)	σ_y	Local stress in the y direction(nN/nm^2)
d_k	length of each cell in the z direction (nm)	σ_z	Local stress in the z direction (nN/nm^2)
a	Nanoparticle diameter (nm)	ν	Poisson's ratio
t	Interphase thickness (nm)	α	Coefficients of thermal expansion(10^{-6}/℃)
d	Nanoparticle length (nm)	ε_y	Local strain in the y direction (nm/nm)
S_x	Global stress in the x direction (nN/nm^2)	ε_z	Local strain in the z direction (nm/nm)
S_y	Global stress in the y direction (nN/nm^2)	ε_x	Local strain in the x direction (nm/nm)
S_Z	Global stress in the z direction (nN/nm^2)		**Subscripts**
E	Elastic modulus (nN/nm^2)	*ijk*	Index of nanocell
ΔT	Temperature deviation (℃)		

results demonstrate rationally good agreement with those of experimental data when nanofillers to be randomly distributed in the polymer matrix and interphase effects to be considered.

Geometry of RVE

Figure 1 describes a model for a nanocomposite material consisting of various regions in the form of nanoparticles enclosed by interphase and randomly distributed in a polymer matrix. Most micromechanical models assume regular nanofiller arrangement and rectangular nanofiller [14-15, 25]. However, in this study in order to consider more realistic nanofiller arrangement and overall behavior prediction of the nanocomposite, it is assumed that the nanofillers are randomly distributed in the polymer matrix. The selected RVE of the nanocomposite consists of $c\times r\times h$ nano-elements in three dimensions with L_h, L_c and L_r as the lengths of the RVE in the *z*, *x* and *y* directions, respectively, as shown in Figure 1.

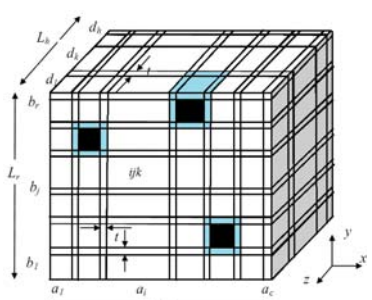

Fig. 1. RVE in the modified SUC model for nanocomposite materials

By letting the counters *i*, *j* and *k* for the *x*, *y* and *z* directions, respectively, each cell is shown as *ijk* and the length of each cell in the *x* direction is a_i, in the *y* direction is b_j and in the *z* direction is d_k. In the selected RVE, *t* is the interphase thickness and *t/a* donates the effective interphase thichness.

A nanoparticle cell of the composite RVE that is enclosed by the interphase is shown in Figure 2. The length of the relevant dimensions of the nano-cell is *a*, *b* and ***d*****.** *a*=*b* is introduced for square cross section of the cell. *d/a* denotes the nanoparticle aspect ratio.

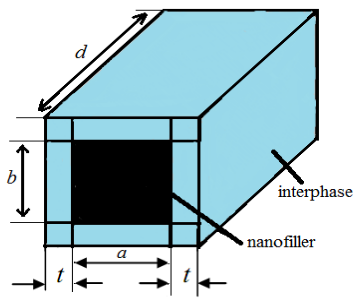

Fig. 2. Cell including nanoparticle

Micromechanical governing equations

According to prior unit cell models [14-17, 25, 31], displacement components are supposed to be linear functions within each sub-cell. Also, it is necessary to assume that the applied normal stresses on the RVE do not introduce shear stress within the sub-cells and vice versa. The equilibrium conditions between applied global stresses (S_l) and local stresses (σ_l^{ijk}) within the sub-cell *ijk* where *l* can be any of *x*, *y* and *z* are:

$$\begin{cases} \sum_{k=1}^{h}\sum_{j=1}^{r} d_k b_j \sigma_x^{1jk} = S_x L_r L_h \\ \sum_{k=1}^{h}\sum_{i=1}^{c} d_k a_i \sigma_y^{i1k} = S_y L_c L_h \\ \sum_{j=1}^{r}\sum_{i=1}^{c} b_j a_i \sigma_z^{ij1} = S_z L_r L_c \end{cases} \quad (1)$$

where a_i, b_j, d_k, L_h, L_c and L_r are shown in Figure 1. The next relationship is obtained from equilibrium of the local stress components along the interfaces of the sub-cells:

$$\begin{cases} \sigma_x^{1jk} = \sigma_x^{ijk} \quad (i>1) \\ \sigma_y^{i1k} = \sigma_y^{ijk} \quad (j>1) \\ \sigma_z^{ij1} = \sigma_z^{ijk} \quad (k>1) \end{cases} \tag{2}$$

The perfect bonding conditions are applied between nanofillers, interphase and matrix.

Thus, compatibility of the displacements within the RVE requires:

$$\begin{cases} \sum_{i=1}^{c} a_i\, \varepsilon_x^{i11} = \sum_{i=1}^{c} a_i\, \varepsilon_x^{ijk} = L_c\, \bar{\varepsilon}_x \quad (j\times k \neq 1) \\ \sum_{j=1}^{r} b_j\, \varepsilon_y^{1j1} = \sum_{j=1}^{r} b_j\, \varepsilon_y^{ijk} = L_r\, \bar{\varepsilon}_y \quad (i\times k \neq 1) \\ \sum_{k=1}^{h} d_k\, \varepsilon_z^{11k} = \sum_{k=1}^{h} d_k\, \varepsilon_z^{ijk} = L_h\, \bar{\varepsilon}_z \quad (i\times j \neq 1) \end{cases} \tag{3}$$

Where ε_l^{ijk} denotes local strains within the sub-cell *ijk* and $\bar{\varepsilon}_l$ denotes global strain where *l* can be any of *x*, *y* and *z*. According to Hooke's law, the 3-D thermo-elastic constitutive equations corresponding to the sub-cell *ijk* can be written as

$$\boldsymbol{\varepsilon}^{ijk} = \mathbf{S}^{ijk}\, \boldsymbol{\sigma}^{ijk} + \boldsymbol{\alpha}^{ijk}\, \Delta T \tag{4}$$

Where σ^{ijk} and ε^{ijk} are the vectors of normal stresses and strains, respectively, S^{ijk} is the elastic compliance matrix, α^{ijk} is the vector of coefficients of thermal expansion, ΔT is the deviation of the temperature from a reference temperature. Substituting equation 4 into equation 3 yields the following relations:

$$\begin{cases} \sum_{i=1}^{c} a_i \{ \frac{1}{E^{i11}}[\sigma_x^{i11} - \nu^{i11}(\sigma_y^{i11} + \sigma_z^{i11})] - \frac{1}{E^{ijk}}[\sigma_x^{ijk} - \nu^{ijk}(\sigma_y^{ijk} + \sigma_z^{ijk})]\} = a_i(\alpha^{ijk} - \alpha^{i11})\Delta T \quad (j\times k \neq 1) \\ \sum_{j=1}^{r} b_j \{ \frac{1}{E^{1j1}}[\sigma_y^{1j1} - \nu^{1j1}(\sigma_x^{1j1} + \sigma_z^{1j1})] - \frac{1}{E^{ijk}}[\sigma_y^{ijk} - \nu^{ijk}(\sigma_x^{ijk} + \sigma_z^{ijk})]\} = b_j(\alpha^{ijk} - \alpha^{i11})\Delta T \quad (i\times k \neq 1) \\ \sum_{k=1}^{h} d_k \{ \frac{1}{E^{11k}}[\sigma_z^{11k} - \nu^{11k}(\sigma_x^{11k} + \sigma_y^{11k})] - \frac{1}{E^{ijk}}[\sigma_z^{ijk} - \nu^{ijk}(\sigma_x^{ijk} + \sigma_y^{ijk})]\} = d_k(\alpha^{ijk} - \alpha^{i11})\Delta T \quad (i\times j \neq 1) \end{cases} \tag{5}$$

Where E^{ijk} and ν^{ijk} are Young's modulus and Poisson's ratio for sub-cell *ijk*, respectively. Using equation 5 in conjunction with equations 1 and 2, a *cr+ch+rh* linear equations system with the same number of unknown is obtained as

$$[\mathbf{A}]_{m\times m}[\boldsymbol{\sigma}]_{m\times 1} = [\mathbf{F}]_{m\times 1} \quad (Where\ m = ch + rh + rc) \tag{6}$$

Where $[\sigma]_{m\times 1}$ is the stress, $[F]_{m\times 1}$ is the external load and $[\mathbf{A}]_{m\times m}$ is the coefficients matrice.

RESULTS AND DISCUSSIONS

The selected composite consist of silica nanoparticles embedded in polyimide matrix. The mechanical and thermal properties of silica and polyimide are listed in Table 1 [32]. Poisson's ratio of interphase is taken equal to that of the polyimide matrix. In order to obtain thermo-elastic properties of the nanocomposite the RVE is extended to 50×50×50 nano-cells.

Table 1
Silica and polyimide properties [32].

	E **(GPa)**	***ν***	***α*** **(°C)**
Silica	88.7	0.23	0.55×10^{-6}
Polyimide	1.679	0.4	30.02×10^{-6}

Effect of volume fraction of nanoparticle

Young's modulus and coefficient of thermal expansion (CTE) of the nanocomposite system versus the volume fraction of nanoparticles are shown in Figures (3-4).

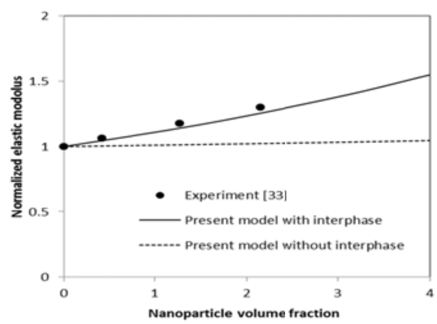

Fig. 3. Variation of elastic modulus with change in volume fraction of silica nanoparticle

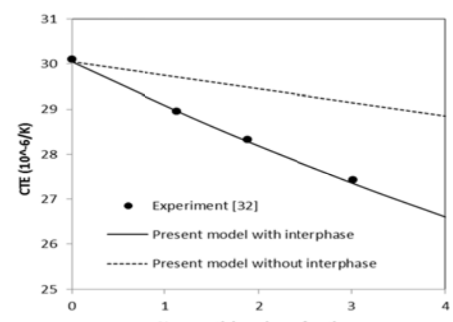

Fig. 4. Variation of CTE with change in volume fraction of silica nanoparticle

Young's modulus and CTE of the interphase material are chosen as E_i=16.79 GPa, and α_i= 22.55×10^{-6}, respectively. Nanoparticle aspect ratio and effective interphase thickness are considered to be 1 and 30/50 nm/nm, respectively. As can be seen in Figures 3 and 4, the proposed micromechanical model with considering interphase effects and random nanoparticle arrangement accurately predicts the experimental data [33].

From theoretical viewpoint, adding silica nanoparticles to the polymer matrix causes an increase in the elastic modulus as compared to that of the pure polymer.

However, from experimental viewpoint, there exists a critical volume fraction beyond which the elastic modulus decreases [34].

This is due to the fact that increasing nanoparticle volume fraction promotes the nanoparticle aggregation.

Furthermore, owning to the formation of the interphase between the nanofillers and matrix with superior material properties than bulk matrix, it would be expected that the three-phase composites at nanoscale (SUC with interphase) present better material properties as compared with those of the two-phase composites (SUC without interphase), as illustrated in Figures (3-4).

Effect of nanoparticle size

A study is performed to investigate the role of nanoparticle size on the thermo-mechanical nanocomposite behavior by increasing the dimension of nanoparticle up to 400 nm.

It is noted that aspect ratio of nanoparticle and the interphase thickness are considered to be 1 and 30 nm, respectively. The volume fraction of nanoparticle is 3%. In Figures (5-6), the elastic modulus and CTE of the nanocomposite are plotted as a function of nanoparticle size. The key role of the interphase on both the elastic modulus and CTE of the nanocomposite is shown.

It can be seen in Figures (5-6) considering the interphase effect, the overall elastic modulus decreases and CTE of the nanocomposite increases as the nanoparticle size increases.

The main reason for this behavior is the reduced influence of the interphase. With decreasing the nanoparticles size, nanoparticles present considerably higher surface to volume ratio which significantly improve their reactivity with surrounding polymer matrix.

Consequently, the interphase region between the nanoparticles and polymer matrix with improved material properties causes an obvious increase in the elastic modulus and reduction in CTE of the nanocomposite.

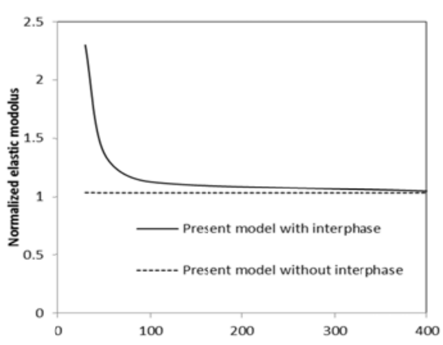

Fig. 5. Effect of nanoparticle size on the elastic modulus of nanocomposite

Effect of nanoparticle aspect ratio

In this subsection, the thermo-mechanical properties of the nanocomposite with change in nanofiller aspect ratio (*d/a*) are extracted.

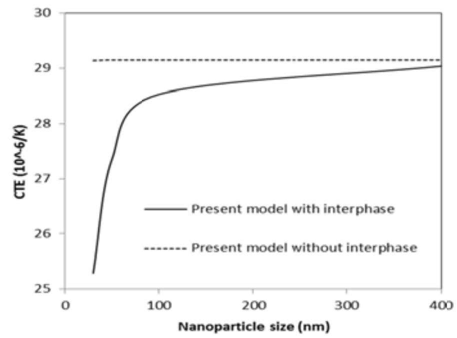

Fig. 6. Effect of nanoparticle size on CTE of nanocomposite

In order to further verify the accuracy of the presented unit cell-based micromechanical model, another comparison is made with the Halpin–Tsai results [23] and experiment [23] for various nanofiller aspect ratios ranging from 1 to 10^4. The considered composite system is nylon-6/clay nanocomposite whose constituents properties have been given in [23]. The comparison results are depicted for the longitudinal elastic modulus in Figure 7.

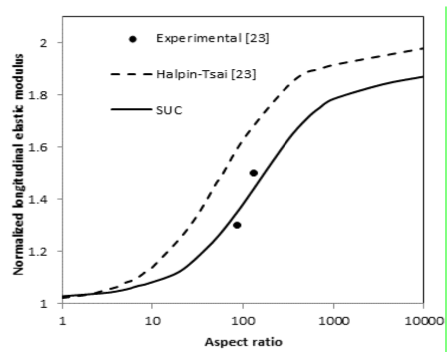

Fig. 7. Variation of longitudinal elastic modulus of nylon-6/clay nanocomposites with change in clay aspect ratio

The interphase thickness and elastic modulus are considered to be 5 nm and $10\times E_m$ (E_m represents the matrix elastic modulus), respectively. It is observed that the SUC model predictions are in close agreement with the experiment It is further observed that the general trend of present results is similar to that of Halpin–Tsai results [23].

As it can be observed in Figure 7, the elastic modulus of the nanocomposite increases with the increase of nanofiller aspect ratio.

It should be noted that the intensity of reinforcement in the nanocomposites is strongly dependent on the aspect ratio of nanofiller.

This underlying phenomenon may be explained by the load-transfer mechanism. In the nanocomposites, the force is transferred between the matrix and nanofillers through their contacting surfaces. Thus, the nanofillers with high aspect ratio that have higher surfaces exhibit higher reinforcement effects.

The SUC model results for the normalized Young's modulus of the nanocomposite with considering effective interphase thickness (*t/a*) equals to 30/50 nm/nm are shown in Figures (8-9) for longitudinal and transverse directions, respectively.

It is obvious that the influences of nanofiller aspect ratio and interphase on longitudinal Young's modulus are significant.

According to Figures (8-9), ignoring interphase effects leads to underestimated predictions of Young's modulus of the nanocomposites.

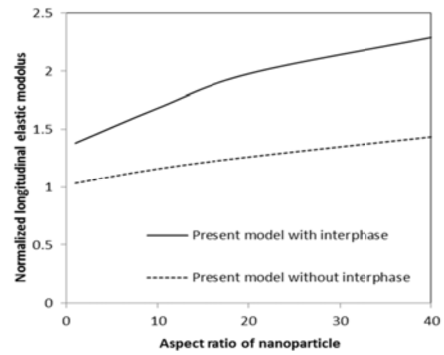

Fig. 8. Variation of longitudinal elastic modulus with change in aspect ratio of silica nanofiller

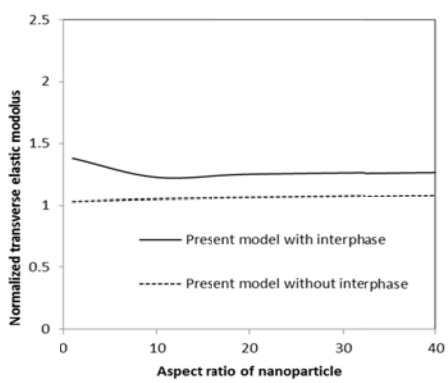

Fig. 9. Variation of transverse elastic modulus with change in aspect ratio of silica nanofiller

Once the interphase effect is considered, the transverse Young's modulus decreases with rising aspect ratio up to 10 and then remains constant.

On the other hand, Compared to nanofiller aspect ratio, the effect of interphase on the transverse Young's modulus is more pronounced, especially when aspect ratio is equal to one.

In Figures (10-11), predictions of CTE of the nanocomposite system in the longitudinal and transverse directions are shown. Figures (10-11) show that nanofiller aspect ratio and the interphase are two factors that play significant role in the prediction of the CTE of the nanocomposite. According to Figures (10-11), ignoring interphase effects leads to overestimated predictions of the CTE of the nanocomposites.

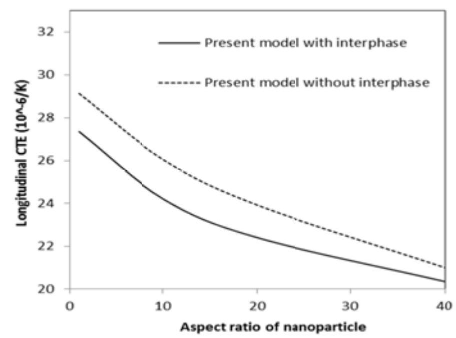

Fig. 10. Variation of longitudinal CTE with change in aspect ratio of silica nanofiller

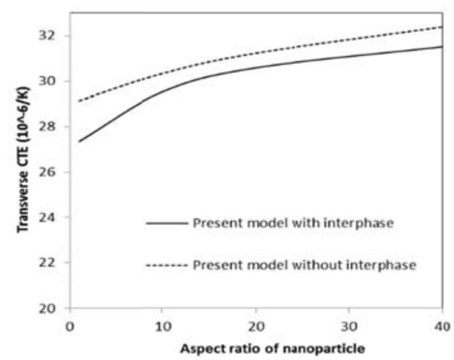

Fig. 11. Variation of transverse CTE with change in aspect ratio of silica nanofiller

Interphase reinforcement ratio

It is obvious that with and without considering interphase, the efficiency of the reinforcement of nanocomposite mechanical properties strongly depends on the nanofillers aspect ratio. Also, it is well-known that the interphase plays a significant role in the nanocomposite materials, but the displayed figures do not provide enough information about the intensity of interphase effect on the final reinforcement in mechanical properties of nanocomposites. Hence, the following formula is introduced to study the intensity of interphase effects on the final reinforcement in mechanical properties of nanocomposites [27]. The goal of such introduction is to separate the effects of interphase from the nanofiller influences. For a composite property (*C*), the interphase reinforcement ratio (*IRR*) is defined as

$$IRR, C = \frac{C_{if} - C_f}{C_f - M} \tag{7}$$

where C_{if} is the composite effective property with considering effects of interphase and fillers, and C_f is the composite effective property without the effects of interphase.

In this equation *M* is matrix property. Equation 7 is presented in order to evaluate the reinforcement of composite material when both interphase and nanofiller effects are considered with respect to the reinforcement of composite material without interphase.

In Figure 12, the obtained *IRR* for Young's modulus are illustrated for different nanofiller aspect ratio. Also, in Figure 13 the obtained *IRR* for Young's modulus are shown for different nanoparticle size with aspect ratio equals to 1. It is noted that volume fraction of nanoparticle is considered to be 3%. As it can be seen in Figure 12, the interphase has the maximum influence in the case of nanocomposite with spherical inclusions. Figure 13 shows that as the nanoparticle size increases, the *IRR* for elastic modulus decreases. This is due to the reduced influence of the interphase.

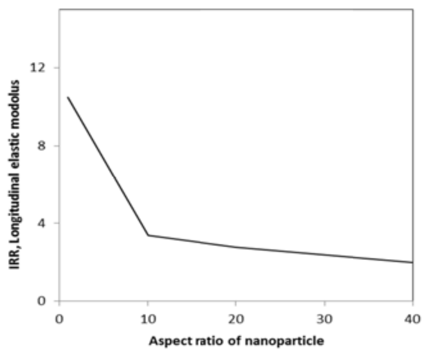

Fig. 12. *IRR* for elastic modulus of nanocomposite for different aspect ratio of nanofiller. Effective interphase thickness is considered to be 30/50 nm/nm

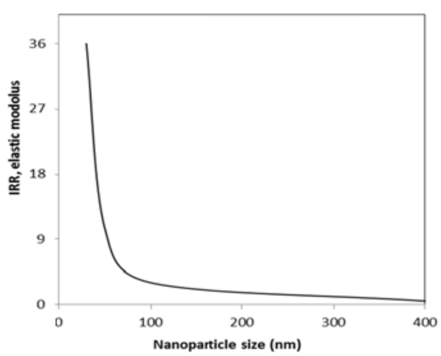

Fig. 13. *IRR* for elastic modulus of nanocomposite for different size of nanofiller. Interphase thickness is considered to be 30 nm

Effects of interphase modulus and interphase thickness

Aspect ratio of nanoparticle is considered to be 1. Figure 14 shows the variation of the Young's modulus of the nanocomposite as a function of Young's modulus of the interphase with considering different effective interphase thicknesses. The nanoparticle volume fraction equals to 3%. Figure 14 indicates that interphase thickness has a significant influence on Young's modulus of the nanocomposite. As shown in this figure, once the interphase Young's modulus increases, Young's modulus of the nanocomposite increases up to a threshold value depending on effective interphase thickness.

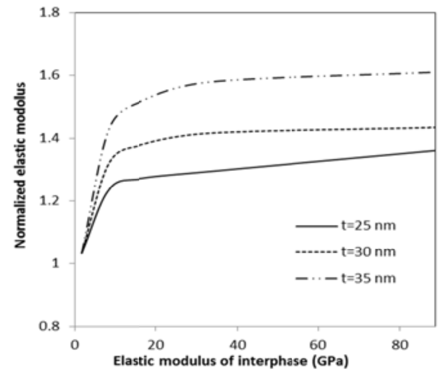

Fig. 14. Variation of the Young's modulus of the nanocomposite as a function of Young's modulus of the interphase with considering different effective interphase thicknesses

Effects of polymer matrix properties

One of the most important factors that affects the interaction between the nanoparticles and matrix is the nature of the polymer matrix. This interaction plays a key role on the expansion of the interphase. Hence, this interaction significantly affects the whole response of nanocomposites. Figure 15 shows the effects of polymer matrix properties on the elastic modulus of nanocomposite.

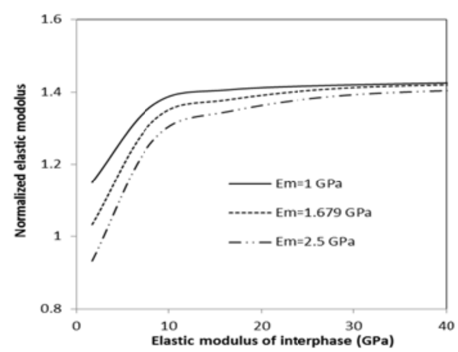

Fig. 15. Effects of polymer matrix properties on the elastic modulus of nanocomposite

In Table 2, a comparison is made between the results of the SUC model code written in MATLAB software) and finite element method (FEM) (simulation carried out by ABAQUS 6.14 package) with considering interphase effect for the elastic modulus of silica nanoparticle-reinforced polyimide nanocomposites.

The table also contains the number of elements together with the CPU time required. A large number of small finite elements are needed in FEM especially between the nanofiller and matrix. The loading and boundary conditions together with the type of elements are similar to Ref. [27]. Since the effective elastic properties of the nanocomposite estimated by the SUC and the FE models are in excellent agreement and the SUC model requires much less computational time than the FE model, one may use the presented SUC approach for intuitive predictions of the effective properties of these nanocomposites, as displayed in Table 2.

Table 2
Comparison between the results of the SUC model and FEM for elastic modulus (GPa) of polyimide nanocomposite reinforced by silica nanoparticles.

	Elastic modulus	Number of elements	Simulation time (sec)
Experiment	2.178	-	-
SUC	2.174	125000	173
FEM	2.175	497308	919

CONCLUSION

In order to study effects of interphase, nanofiller geometry and matrix properties on the response of nanocomposites, a three-dimensional micromechanics-based analytical model was developed. The most important advantages of this new model are its accuracy, simplicity, and efficiency. The geometry of the new RVE of the modified simplified unit cell model was extended to $c\times r\times h$ sub-cells in three dimensions. The interphase was introduced as a third phase around the nanoparticles in the nanocomposite modeling. Results of the modified version of SUC model were compared with experimental data. These comparisons demonstrate that the presented model is capable of providing precise predictions for the thermo-elastic properties of nanocomposites. Results show that for nanocomposite structures, interphase presents the maximum effect for spherical nanoparticles (aspect ratio equals to one). For the interphase elastic stiffness a threshold value depending on interphase thickness was observed. Also, significant improvement in thermo-mechanical properties was observed with decreasing nanoparticle size.

REFERENCES

[1] B.M. Novak: Hybrid nanocomposite materials-between inorganic glasses and organic polymers, Adv Mater 5 (1993) 422-433.

[2] H.L. Frisch, J.E. Mark: Nano composites prepared by threading polymer chains through zeolites, mesoporous silica, or Silica nanotubes, Chem Mater 8 (1996) 1735-1738.

[3] B. Wetzel, F. Haupert, M.Q. Zhang: Epoxy nano composites with high mechanical and tribological performance, Compos Sci Technol 63 (2003) 2055–2067.

[4] H. Wang, Y. Bai, S. Liu, J. Wu, C.P. Wong: combined effects of silica filler and its interface in epoxy resin, Acta Mater 50 (2002) 4369–4377.

[5] J.N. Coleman, M. Cadek, R. Blake, V. Nicolosi, K.P. Ryan, C. Belton, A. Fonseca, J.B. Nagy, Y.K. Gun'ko, W. J. Blau: High-performance nanotube-reinforced plastics: understanding the mechanism of strength increase, Adv Func Mater 14 (2004) 791–798.

[6] M. Izadi, M.M. Shahmardan, A. Behzadmehr, A.M. Rashidi, A. Amrollahi: Modeling of effective thermal conductivity and viscosity of carbon structured nanofluid, Trans Phenom in Nano Micro scale 3 (2015) 1-13.

[7] G.D. Seidel, D.C. Lagoudas: A micromechanics model for the electrical conductivity of nanotube-polymer nanocomposites, J Compos Mater 43 (2009) 917–941.

[8] H. Liu, L.C. Brinson: Reinforcing efficiency of nanoparticles: A simple comparison for polymer nanocomposites, Compos Sci Technol 68 (2008) 1502-1512.

[9] L.S. Schadler, L.C. Brinson, W.G. Sawyer: Polymer Nanocomposites: A Small Part of the Story, J Miner Metal Mater Soc 59 (2007) 53-60.

[10] M. Avella, F. Bondioli, V. Cannillo, M.E. Errico, A. M. Ferrari, B. Focher, M. Malinconico, T. Manfredini, M. Montorsi: Preparation, characterisation and computational study of poly (e-caprolactone) based nanocomposites, Mater Sci Technol 20 (2004a) 1340–1344.

[11] M. Avella, F. Bondioli, V. Cannillo, S. Cosco, M.E. Errico, A.M. Ferrari, B. Focher, M. Malinconico: Properties/structure relationships in innovative PCL–SiO_2 nanocomposites, Macromol Symp 218 (2004b) 201–210.

[12] L.S. Schadler: Designed Interfaces in Polymer Nanocomposites: A Fundamental Viewpoint, MRS Bulletin 32 (2007) 335-340.

[13] R.A. Vaia, H.D. Wagner: Framework for Nanocomposites, Mater Today 7 (2004) 32-37.

[14] J.S. Snipes, C.T. Robinson, S.C. Baxter: Effects of scale and interface on the three-dimensional micromechanics of polymer nanocomposites, J Compos Mater 45 (2011) 2537-2546.

[15] S.C. Baxter, C.T. Robinson: Pseudo-percolation: Critical volume fractions and mechanical percolation in polymer nanocomposites, Compos Sci Technol 71 (2011) 1273–1279.

[16] M.J. Mahmoodi, M.M. Aghdam: Damage analysis of fiber reinforced Ti-alloy subjected to multi-axial loading—A micromechanical approach, Mater Sci Eng A 528 (2011) 7983-7990.

[17] S.R . Falahatgar, M. Salehi, M.M. Aghdam: Non-linear viscoelastic response of unidirectional fiber reinforced composites in off-axis loading, J Reinf Plast Compos 28 (2009)1793–1812.

[18] R.P. Nimmer, R.J. Bankert, E.S. Russell, G.A. Smith, P.K. Wright: Micromechanical modeling of

fiber/matrix interface effects in transversely loaded SiC/Ti-6-4 metal matrix composite, J Compos Technol Res 13 (1991) 3-13.
[19] R. Haj-Ali, J. Aboudi: Nonlinear micromechanical formulation of the high fidelity generalized method of cells, Int J Solids Struct 46 (2009) 2577-2592.
[20] T.W. Chou, S. Nomura, M. Taya: A self-consistent approach to the elastic stiffness of short-fiber composites, J Compos Mater 14 (1980) 178-188.
[21] J.C. Halpin, S.W. Tsai: Stiffness and expansion estimates for oriented short fiber composites, J Compos Mater 3 (1969) 732–734.
[22] T. Mori, K. Tanaka: Average stress in matrix and average elastic energy of materials with misfitting inclusions, Acta Metal 21 (1973) 571-574.
[23] J.I. Weon, H.J. Sue: Effects of clay orientation and aspect ratio on mechanical behavior of nylon-6 nanocomposite, Polymer 46 (2005) 6325–6334.
[24] H.W. Wang, H.W. Zhou, R.D. Peng, J. Leon Mishnaevsky: Nanoreinforced polymer composites: 3D FEM modeling with effective interface concept, Compos Sci Technol 71 (2011) 980–988.
[25] S. Dhala, M.C. Ray:Micromechanics of piezoelectric fuzzy fiber-reinforced composite, Mech Mater 81 (2015) 1–17.
[26] R.D. Peng, H.W. Zhou, H.W. Wang, J. Leon Mishnaevsky: Modeling of nano-reinforced polymer composites: Microstructure effect on Young's modulus, Comput Mater Sci 60 (2012) 19–31.
[27] B. Mortazavi, J. Bardon, S. Ahzi: Interphase effect on the elastic and thermal conductivity response of polymer nanocomposite materials: 3D finite element study, Comput Mater Sci 69 (2013) 100–106.
[28] S. Ajori, R. Ansari, M. Mirnezhad: Mechanical properties of defective γ-graphyne using molecular dynamics simulations, Mater Sci Eng: A 561 (2013) 34–39.
[29] R. Ansari, S. Rouhi, S. Ajori: Elastic properties and large deformation of two-dimensional silicene nanosheets using molecular dynamics, Super Microstruct 65 (2014) 64–70.
[30] M.M. Shokrieh, R. Rafiee: Development of a full range multi-scale model to obtain elastic properties of CNT/polymer composites, Iran Polymer J 21 (2012) 397-402.
[31] M.J. Mahmoodi, M.M. Aghdam, M. Shakeri: The effects of interfacial debonding on the elastoplastic response of unidirectional silicon carbide–titanium composites, J Mech Eng Sci 223 (2010) 259-269.
[32] Z. Wanga, J. Lua, Y. Li, S.Y. Fu, S. Jiang, X. Zhao: Studies on thermal and mechanical properties of PI/SiO_2 nanocomposite films at low temperature, Composites A 37 (2006) 74–79.
[33] G.M. Odegard, T.C. Clancy, T.S. Gates: Modeling of the mechanical properties of nanoparticle/polymer composites, Polymer 46 (2005) 553–562.
[34] E. Kontou, G. Anthoulis:The effect of silica nanoparticles on the thermomechanical properties of polystyrene, J. Appl. Polym. Sci 105 (2007) 1723–1731.